thereby facilitating reduction of polyoxometallates of these types.

The concept of binodal orbital aromaticity in reduced early-transition-metal polyoxometallates may be related to their classification as mixed valence compounds. Robin and Day[36] classify mixed valence compounds into the following three classes: Class I, fully localized corresponding to an insulator in an infinite system; Class II, partially delocalized corresponding to a semiconductor in an infinite system; and Class III, completely delocalized corresponding to a metal in an infinite system. ESR studies on the one-electron reduced polyoxometallates $M_6O_{19}^{n-}$ and $XM_{12}O_{40}^{n-}$ suggest class II mixed valence species.[37,38] Although such species are delocalized at accessible temperatures, they behave as localized systems at sufficiently low temperatures similar to semiconductors. This is in accord with the much smaller overlap (i.e., lower β in eq 5) of the metal d_{xy} orbitals associated with binodal orbital aromaticity as compared with the boron sp hybrid anodal internal orbitals in the deltahedral boranes $B_nH_n^{2-}$ or the carbon uninodal p orbitals in benzene.

REFERENCES AND NOTES

(1) Paper presented to the American Chemical Society Division of Computers in Chemistry at the Symposium on *Chemical Applications of Graph Theory* in conjunction with the Fourth Chemical Congress of North America, New York, Aug 1991.
(2) Streitwieser, A., Jr. *Molecular Orbital Theory for Organic Chemists*; Wiley: New York, 1961.
(3) Salem, L. *The Molecular Orbital Theory of Conjugated Systems*; Benjamin: New York, 1966.
(4) Dewar, M. J. S. *The Molecular Orbital Theory of Organic Chemistry*; McGraw-Hill: New York, 1969.
(5) Aihara, J. *Bull. Chem. Soc. Jpn.* **1975**, *48*, 517.
(6) Aihara, J. *Bull. Chem. Soc. Jpn.* **1975**, *48*, 1501.
(7) Aihara, J. *J. Am. Chem. Soc.* **1976**, *98*, 2750.
(8) Wade, K. *Chem. Commun.* **1971**, 792.
(9) Mingos, D. M. P. *Nature (London), Phys. Sci.* **1972**, *236*, 99.
(10) Wade, K. *Adv. Inorg. Chem. Radiochem.* **1976**, *18*, 1.
(11) Mingos, D. M. P. *Acc. Chem. Res.* **1984**, *17*, 311.
(12) Ceriotti, A.; Demartin, F.; Heaton, B. T.; Ingallina, P.; Longoni, G.; Manassero, M.; Marchionna, M.; Masciocchi, N. *Chem. Commun.* **1989**, 786.
(13) King, R. B. *Inorg. Chem.* **1991**, *30*, 4437.
(14) King, R. B. *J. Math. Chem.* **1987**, *1*, 249.
(15) Behzad, M.; Chartrand, G. *Introduction to the Theory of Graphs*; Allyn and Bacon: Boston, 1971; section 1.1.
(16) Grünbaum, B. *Convex Polytopes*; Interscience: New York, 1967.
(17) Ruedenberg, K. *J. Chem. Phys.* **1954**, *22*, 1878.
(18) Schmidtke, H. H. *J. Chem. Phys.* **1966**, *45*, 3920.
(19) Schmidtke, H. H. *Coord. Chem. Rev.* **1967**, *2*, 3.
(20) Gutman, I.; Trinajstić, N. *Top. Curr. Chem.* **1973**, *42*, 49.
(21) Biggs, N. L. *Algebraic Graph Theory*; Cambridge University Press: London, 1974; p 9.
(22) King, R. B.; Rouvray, D. H. *J. Am. Chem. Soc.* **1977**, *99*, 7834.
(23) King, R. B. In *Chemical Applications of Topology and Graph Theory*; King, R. B., Ed.; Elsevier: Amsterdam, 1983; pp 99-123.
(24) King, R. B. In *Molecular Structure and Energetics*; Liebman, J. F., Greenberg, A., Eds.; VCH: Deerfield Beach, FL, 1976; pp 123-148.
(25) King, R. B. *Rep. Mol. Theor.* **1990**, *1*, 141.
(26) Wilson, R. J. *Introduction to Graph Theory*; Oliver and Boyd: Edinburgh, 1972; p 16.
(27) King, R. B. *J. Comput. Chem.* **1987**, *8*, 341.
(28) Hoffmann, R.; Lipscomb, W. N. *J. Chem. Phys.* **1962**, *36*, 2179.
(29) Pope, M. T. *Heteropoly and Isopoly Oxometallates*; Springer-Verlag: Berlin, 1983.
(30) Day, V. W.; Klemperer, W. G. *Science* **1985**, *228*, 533.
(31) Launay, J. P.; Babonneau, F. *Chem. Phys.* **1982**, *67*, 295.
(32) Cairns, C. J.; Busch, D. H. *Coord. Chem. Rev.* **1986**, *69*, 1.
(33) Ref 21, p 14.
(34) Prados, R. A.; Pope, M. T. *Inorg. Chem.* **1976**, *15*, 2547.
(35) Varga, G. M., Jr.; Papaconstantinou, E.; Pope, M. T. *Inorg. Chem.* **1970**, *9*, 662.
(36) Robin, M. B.; Day, P. *Adv. Inorg. Chem. Radiochem.* **1967**, *10*, 247.
(37) Lennay, J. P.; Fournier, M.; Sanchez, C.; Livage, J.; Pope, M. T. *Inorg. Nucl. Chem. Lett.* **1980**, *16*, 257.
(38) Barrows, J. N.; Pope, M. T. *Adv. Chem. Ser.* **1990**, *226*, 403.

Combinatorics of Cluster Enumeration

K. BALASUBRAMANIAN†

Department of Chemistry, Arizona State University, Tempe, Arizona 85287-1604

Received August 27, 1991

Recent developments in the enumeration of isomers of gallium arsenide clusters of the formula Ga_xAs_y as well as hydrogenated clusters of C_{60} such as $C_{60}H_n$ and deuterated clusters $C_{60}H_nD_m$ are reviewed. The procedures for the combinatorical enumeration of isomers of $C_{60}H_nX_m$ are also outlined. The nuclear spin statistics and the classification of rotational levels of $C_{60}H_{60}$ and $C_{60}D_{60}$ are considered using combinatorical methods.

1. INTRODUCTION

Clusters have been the topic of an increasing number of theoretical and experimental studies in recent years.[1-23] The increased interest stems from several experimental studies. The first and also the most important investigation from the standpoint of impact is the synthesis and characterization of the "buckminsterfullerene" or the C_{60} clusters.[6-8] The aesthetically appealing soccerball-shaped cluster generated intense experimental and theoretical activity on the topic. The theoretical studies included numerous semiempirical and ab initio studies as well as topological characterization of related clusters. The C_{60} cluster also revived the resonance theory of polycyclic molecules containing carbon atoms. The C_{60} cluster also generated topological interest on other forms of platonic solids.

The recent synthesis of gram quantities of C_{60} as well as $C_{60}H_{36}$, $C_{60}H_{60}$, and other molecules[21] generated by the Birch reduction has provided significant impetus for the ab initio and graph theoretical studies for the hydrogenated C_{60} cluster.

Another interesting set of clusters of great importance in the semiconductor area is the cluster of gallium arsenide of the general formula, Ga_xAs_y. O'Brien et al.[1] produced these clusters using the laser vaporization of pure GaAs crystal. A fascinating finding of O'Brien et al. is that the smaller clusters deviated significantly from the binomial distribution of relative abundance while the large clusters followed a binomial distribution. It is not evident whether the strong deviation displayed by the smaller clusters is due to inherent extra stability (magic numbers) or if this is due to the possibility of greater number of isomers (long-lived) with that particular molecular formula.

Ab initio cluster computations also require often-possible structures for a given cluster. Codes which do not have automated geometry optimization techniques especially require as input possible geometries for energetics consideration.

The experimentally observed fragmentation patterns for clusters are also very intriguing. The explanation of the

† Camille and Henry Dreyfus Teacher-Scholar.

0095-2338/92/1632-0047$03.00/0

photofragmentation patterns require consideration of alternative fragmentation channels and the energetics of each such channel. In all of the above applications to explain baffling experimental phenomena, the first step would be combinatorial considerations. Combinatorics deal with possible ways of constructing configurations with a given set of constraints. It involves enumeration, construction, characterization, and optimization. The objective of this article is to outline enumerative combinatorics of clusters. Often the enumerative techniques when combined with the energetics criteria could lead to important clues to unravel experimental mysteries. Section 2 outlines the basic enumerative combinatorics based on generalized character cycle indices. Section 3 considers applications to Ga_xAs_y, while section 4 outlines applications to $C_{60}H_n$ and $C_{60}H_nD_m$, etc. Section 5 considers the nuclear spin statistics of $C_{60}H_{60}$ and $C_{60}D_{60}$.

2. COMBINATORIAL METHODS

I[36,37] have introduced a generator called the generalized character cycle index (GCCI), which is a very useful generator for the enumeration of structures, irreducible representations, and nuclear spin functions. The GCCIs have numerous applications in NMR, electronic structure calculations, NQR, ESR, molecular spectroscopy, etc. The readers are referred to the review in ref 25 on the topic. In this article the focus is on the applications of the GCCI to enumerate isomers and for the generation of nuclear spin statistical weights of clusters.

The GCCI which corresponds to the character $\chi: g \rightarrow \chi(g)$ of an irreducible representation Γ in the group G, $g \in G$, is given by

$$P_G^{\chi} = \frac{1}{|G|} \sum_{g \in G} \chi(g) x_1^{b_1} x_2^{b_2} \ldots$$

A special case of the GCCI for the identity-irreducible representation A_1 whose character $\chi: g \rightarrow 1$ for all g is given by

$$P_G = \frac{1}{|G|} \sum_{g \in G} x_1^{b_1} x_2^{b_2} \ldots x_n^{b_n}$$

The above expression for the identity character is the cycle index of a group G introduced by Pólya[28] for the enumeration of isomers.

Suppose F is a set of all functions from a set D to another set R. D may be the set of vertices in the chemical graph, and R may be the set of substituents (colors). In another application D may be the set of nuclei, and R may be the set of possible nuclear spin projections for a nucleus in the set D. One can construct $|R|^{|D|}$ possible maps from the set D to R, where $|R|$ and $|D|$ are the number of elements in the respective sets.

Suppose with each element $r \in R$, we associate a weight $w(r)$, then we can obtain the number of times a given irreducible representation Γ occurs in the set F of all functions using the GCCI as follows:

$$GF^{\chi} = P_G^{\chi}[x_k \rightarrow \sum_{r \in R} [w(r)]^k]$$

where GF^{χ} is known as the generating function associated with the irreducible representation Γ, the arrow symbol stands for replacing every x_k in the GCCI with sum of the kth powers of weights in the set R. The special case of χ being the character of the totally symmetric representation is the well-known Pólya's theorem,[28] which has been successfully employed in numerous applications involving conventional isomers of organic molecules and inorganic complexes (see my review[25]).

The applications of the GCCI to clusters is relatively a new topic. We show in this article that such applications could provide important information pertaining to cluster distribution, fragmentation and possible isomers, and nuclear spin statistics of clusters.

3. APPLICATION TO THE ISOMERS OF GA_XAS_Y

I[32] applied the partition generating function method and Pólya's theorem to enumerate the possible isomers of Ga_xAs_y. Note that King[38] has used the concept of partitions to construct the chirality polynomials. Possible structures with a given electron count have also been constructed in the literature.[39] Following my prediction of the isomers of Ga_xAs_y, the experimental studies by Reents[34] as well as Mandich and coworkers[35] have confirmed the existence of isomers for these clusters. In this section, the combinatorial procedures used for the enumeration of Ga_xAs_y clusters are described. The construction of most interesting polyhedra can be simplified by considering the possible equivalence classes of the vertices of the polyhedra. For example, all five vertices are equivalent for a pentagon, while for a square pyramid the apex vertex is not equivalent to the base vertices. Likewise, the trigonal bipyramid has two equivalence classes of vertices, namely, the axial and equatorial vertices.

The equivalence classes of n objects correspond to the possible partitions of the integer n. For example, the possible partitions of the integer 5 are 5, 4 + 1, 3 + 2, 3 + 1 + 1, 2 + 2 + 1, 2 + 1 + 1 + 1, and 1 + 1 + 1 + 1 + 1. The number of partitions of an integer n into p parts (P_n^p) is generated by the coefficient of x^n in the expression

$$F(x) = x^p(1 - x)^{-1}(1 - x^2)^{-1} \ldots (1 - x^p)^{-1}$$

The P_n^m's are also given by the following recursive relation:

$$P_{n+m}^m = P_n^1 + P_n^2 + P_n^3 + \ldots + P_n^m$$

If one considers each partition of n as a partition of the vertices of polyhedron, then the possible polyhedra for that partition of vertices could be constructed by using intuitive arguments. For example, possible polyhedra for the partition 4 of our vertices are regular tetrahedra and rhombus. Note that a square is a special case of rhombus. Likewise, for the partition 3 + 1, a triangular pyramid would be a possibility. For the partition 2 + 2, one could assign a linear or a trapezoidal structure. The 1^n partition corresponds to a totally distorted structure and was not considered. For some partitions, it might be difficult to find an interesting structure. The partitions of n were thus used as a guide to construct the possible interesting parent polyhedra.

If w_1 and w_2 denote the weights for gallium and arsenic atoms, then a generating function (GF) which is a polynomial in w_1 and w_2 can be obtained by the following substitution in the GCCI of the identity representation:

$$GF = P_G(x_k \rightarrow w_1^k + w_2^k)$$

where the arrow stands for replacing every x_k in P_G by $w_1^k + w_2^k$.

The group G is taken to be the rotational subgroup of the point group of the polyhedron since enantiomers are also enumerated. To exemplify this consider the rotational subgroup of the cube shown below:

$$P_G = \frac{1}{24}(x_1^8 + 6x_4^2 + 9x_2^4 + 8x_1^2x_3^2)$$

Replacing every x_k in the above expression by $w_1^k + w_2^k$ yields

$$GF = \frac{1}{24}[(w_1 + w_2)^8 + 6(w_1^4 + w_2^4)^2 + 9(w_1^2 + w_2^2)^4 + 8(w_1 + w_2)^2(w_1^3 + w_2^3)^2]$$

which when simplified results in

$$w_1^8 + w_1^7w_2 + 3w_1^6w_2 = 3w_1^5w_2^3 + 7w_1^4w_2^4 + 3w_1^3w_2^5 + 3w_1^2w_2^6 + w_1w_2^7 + w_2^8$$

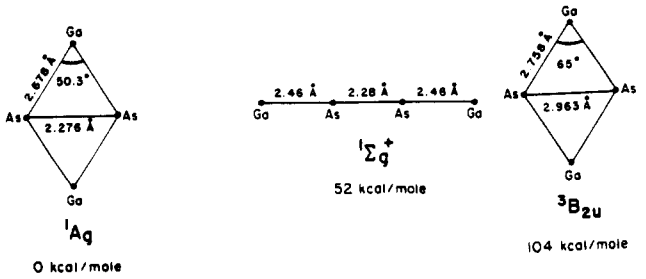

Figure 1. Geometries of electronic states of Ga_2As_2 from ab initio studies.

The coefficient of $w_1^m w_2^n$ in the above expression enumerates the number of isomers of Ga_mAs_n that have cubic polyhedral structure. Consequently, there is one Ga_8 isomer, one Ga_7As isomer, three Ga_6As_2 isomers, etc., with cubic structure.

Table I shows a selected list of vertex partitions, the polyhedral forms, the point group of the polyhedron, and the corresponding generating functions. Note that Table I is not exhaustive. The only polyhedron with 12 vertices considered was an icosahedron. The actual probable polyhedral form for a given isomer would be determined by many factors such as electron counts, stability criterion, bond lengths, Jahn–Teller distortions, imaginary vibrational frequencies, etc.

Among tetramers the rhombus, trapezoidal, and linear forms exhibit isomerism. There are two possible isomers for Ga_2As_2 with the rhombus structure while there are four isomers for the trapezoidal form. Since the As–As bond length is much shorter than the Ga–Ga bond length, the shorter side of the trapezium is occupied by the arsenic atoms while the longer side is occupied by the gallium atoms. In the rhombus structure, the As–As diagonal is considerably shorter than the Ga–Ga diagonal, thereby stabilizing the structure through As–As and four Ga–As bonds. The actual bond length considerations predict that the rhombus structure is favored if the Ga atoms are diagonally across each other and the trapezoidal structure is preferred if the gallium atoms are next to each other. This was subsequently confirmed by two ab initio calculations.[33,40] The ab initio structures computed are in Figure 1.

O'Brien et al.[1] generated Ga_xAs_y clusters through the laser vaporization of GaAs crystal to explain the strong deviation of the dimer. The mass analysis of the generated clusters indicated that the relative abundance of smaller clusters strongly deviated from a binomial distribution but the larger clusters were followed by a binomial distribution. Since As_2 is very stable compared to GaAs and Ga_2, the dimers were dominated by As_2. The experimental abundance of the trimers was found to be 50% As_3 and 30% $GaAs_2$. The generating function for trimers is given by

$$w_1^3 + 2w_1^2w_2 + 2w_1w_2^2 + w_2^3$$

This expression suggests that there are two isomers for $GaAs_2$ and Ga_2As. The generating function thus obtained indicates that the probability of forming $GaAs_2$ should be as twice as that of forming As_3, and the relative strengths of the As–As and Ga–As bonding should be the same. But $GaAs_2$ contains two Ga–As bonds and one As–As bond, while As_3 contains three As–As bonds. If the probabilities are multiplied with the approximate ratios of the D_e's of the two species (As_2, GaAs) then the ratio of the probability for forming As_3 and $GaAs_2$ comes out to be 1.4, which is not very far from the observed distribution of As_3 (50%) and $GaAs_2$ (30%). A weighted distribution obtained from the generating function and using approximate bond strengths is

$$As_3\ (51\%),\ GaAs_2\ (37\%),\ Ga_2As\ (9\%),\ Ga_3\ (3\%)$$

The above distribution is close to the observed distribution of

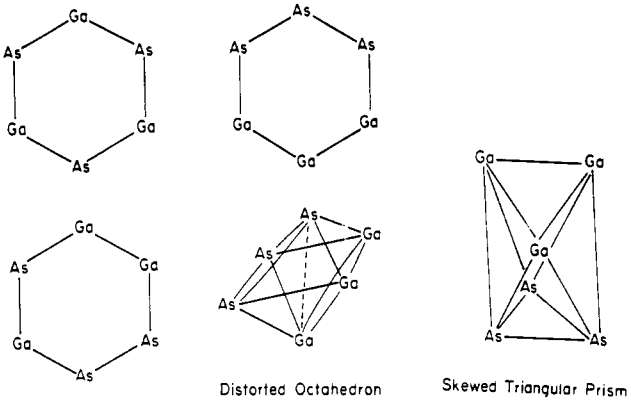

Figure 2. Some isomers for Ga_3As_3. In the hexagonal structure, isomer with alternating Ga and As atoms is energetically favored.

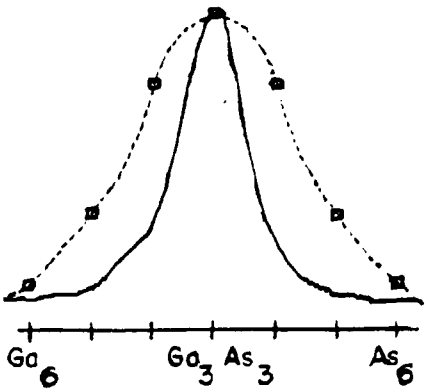

Figure 3. Observed and binomial distributions for Ga_xAs_y ($x + y = 6$).

trimers. Again, the tetramers are overrepresented by Ga_2As_2 and $GaAs_3$.

The coefficient of the $w_1^3w_2^3$ term is the largest for six-atom clusters in various forms (Table I). Although only a few forms in Table I are attractive candidates, all forms in Table I contain larger coefficients for the $w_1^3w_2^3$ terms. Possible candidates for Ga_3As_3 stable isomers from Table I are the skewed triangular prism (three As on one side and three Ga on the other side), planar hexagon with alternating Ga and As atoms, distorted octahedron et al. (some of these are shown in Figure 2).

Figure 3 shows the distribution observed by O'Brien et al.[1] for six-atom clusters and the binomial distribution (expected). Experimentally, Ga_3As_3 is considerably more abundant (70%) for the six-atom clusters than what is predicted by the binomial distribution. Hence the possible sources for the stronger Ga_3As_3 peak are (i) more than one possible long-lived isomer in the beam and (ii) enhanced stability of Ga_3As_3 compared to other six-atom clusters since combinatorics favors a larger number of Ga–As bonds in this structure than any other structure for the six-atom clusters.

4. ENUMERATION OF ISOMERS OF $C_{60}H_N$, $C_{60}H_ND_M$, ETC.

Our enumeration of isomers of hydrogenated C_{60} was motivated by the synthesis of $C_{60}H_{36}$ and other molecules by Smalley and co-workers[20] using the Birch reduction. Figure 4 shows the buckminsterfullerene C_{60} molecule. The point group of this structure is I_h, and thus the cycle index of the rotational subgroup I for the set of sixty vertices in Figure 4 is constructed. This is shown as

$$P_I = 1/60[x_1^{60} + 24x_5^{12} + 20x_3^{20} + 15x_2^{30}]$$

Suppose D is the set of 60 vertices in Figure 4 and R is the set of colors such as white, green, blue, etc. in the set. Practical

Table I. Generating Functions for Isomers of Ga_xAs_y Clusters

n	P_n	G	polyhedron	GF
4	4	T_d	tetrahedron	$w_1^4 + w_1^3w_2 + w_1^2w_2^2 + w_1w_2^3 + w_2^4$
4	4	D_{4h}	rhombus	$w_1^4 + w_1^3w_2 + 2w_1^2w_2^2 + w_1w_2^3 + w_2^4$
4	3 + 1	C_{3v}	triangular pyramid	$w_1^4 + 2w_1^3w_2 + 2w_1^2w_2^2 + 2w_1w_2^3 + w_2^4$
4	2 + 2	C_{2v}	linear	$w_1^4 + 2w_1^3w_2 + 4w_1^2w_2^2 + 2w_1w_2^3 + w_2^4$
4	2 + 2	C_{2v}	trapezoid	$w_1^4 + 2w_1^3w_2 + 4w_1^2w_2^2 + 2w_1w_2^3 + w_2^4$
5	5	D_{5h}	pentagon	$w_1^5 + w_1^4w_2 + 2w_1^3w_2^2 + 2w_1^2w_2^3 + w_1w_2^4 + w_2^5$
5	4 + 1	C_{4v}	square pyramid	$w_1^5 + 2w_1^4w_2 + 3w_1^3w_2^2 + 3w_1^2w_2^3 + 2w_1w_2^4 + w_2^5$
5	4 + 1	T_d	tetrahedron with central atom	$w_1^5 + 2w_1^4w_2 + 2w_1^3w_2^2 + 2w_1^2w_2^3 + 2w_1w_2^4 + w_2^5$
5	3 + 2	D_{3h}	tbp	$w_1^5 + 2w_1^4w_2 + 3w_1^3w_2^2 + 3w_1^2w_2^3 + 2w_1w_2^4 + w_2^5$
5	3 + 1 + 1	C_{3v}	distorted tbp	$w_1^5 + 3w_1^4w_2 + 4w_1^3w_2^2 + 4w_1^2w_2^3 + 3w_1w_2^4 + w_2^5$
5	2 + 2 + 1	C_{2v}	polarized tbp	$w_1^5 + 3w_1^4w_2 + 6w_1^3w_2^2 + 6w_1^2w_2^3 + 3w_1w_2^4 + w_2^5$
5	2 + 2 + 1	C_{2v}	linear	$w_1^5 + 3w_1^4w_2 + 6w_1^3w_2^2 + 6w_1^2w_2^3 + 3w_1w_2^4 + w_2^5$
5	3 + 1 + 1	C_{3v}	capped tetrahedron	$w_1^5 + 3w_1^4w_2 + 4w_1^3w_2^2 + 4w_1^2w_2^3 + 3w_1w_2^4 + w_2^5$
6	6	D_{6h}	hexagon	$w_1^6 + w_1^5w_2 + 3w_1^4w_2^2 + 3w_1^3w_2^3 + 3w_1^2w_2^4 + w_1w_2^5 + w_2^6$
6	6	D_{3h}	trigonal prism	$w_1^6 + w_1^5w_2 + 4w_1^4w_2^2 + 4w_1^3w_2^3 + 4w_1^2w_2^4 + w_1w_2^5 + w_2^6$
6	6	D_{3d}	trigonal antiprism	$w_1^6 + w_1^5w_2 + 4w_1^4w_2^2 + 4w_1^3w_2^3 + 4w_1^2w_2^4 + w_1w_2^5 + w_2^6$
6	6	O_h	octahedron	$w_1^6 + w_1^5w_2 + 2w_1^4w_2^2 + 2w_1^3w_2^3 + 2w_1^2w_2^4 + w_1w_2^5 + w_2^6$
6	5 + 1	C_{5v}	pentagonal pyramid	$w_1^6 + 2w_1^5w_2 + 3w_1^4w_2^2 + 4w_1^3w_2^3 + 3w_1^2w_2^4 + 2w_1w_2^5 + w_2^6$
6	4 + 2	D_{4h}	square bP	$w_1^6 + 2w_1^5w_2 + 4w_1^4w_2^2 + 4w_1^3w_2^3 + 4w_1^2w_2^4 + 2w_1w_2^5 + w_2^6$
6	2 + 2 + 2	C_{2v}	bicapped tetrahedron	$w_1^6 + 3w_1^5w_2 + 9w_1^4w_2^2 + 10w_1^3w_2^3 + 9w_1^2w_2^4 + 3w_1w_2^5 + w_2^6$
6	2 + 2 + 2	C_{2v}	tri-distorted octahedron	$w_1^6 + 3w_1^5w_2 + 9w_1^4w_2^2 + 10w_1^3w_2^3 + 9w_1^2w_2^4 + 3w_1w_2^5 + w_2^6$
6	2 + 2 + 2	C_{2v}	bicapped tetrahedron	$w_1^6 + 3w_1^5w_2 + 9w_1^4w_2^2 + 10w_1^3w_2^3 + 9w_1^2w_2^4 + 3w_1w_2^5 + w_2^6$
6	2 + 2 + 1 + 1	C_{2v}	edge-capped TbP	$w_1^6 + 4w_1^5w_2 + 9w_1^4w_2^2 + 12w_1^3w_2^3 + 9w_1^2w_2^4 + 4w_1w_2^5 + w_2^6$
7	7	D_{7h}	regular heptagon	$w_1^7 + w_1^6w_2 + 3w_1^5w_2^2 + 4w_1^4w_2^3 + 4w_1^3w_2^4 + 3w_1^2w_2^5 + 3w_1w_2^6 + w_2^7$
7	6 + 1	C_{6v}	hexagonal pyramid	$w_1^7 + 2w_1^6w_2 + 4w_1^5w_2^2 + 7w_1^4w_2^3 + 7w_1^3w_2^4 + 4w_1^2w_2^5 + 2w_1w_2^6 + w_2^7$
7	5 + 2	D_{5h}	pentagonal bipyramid	$w_1^7 + 2w_1^6w_2 + 4w_1^5w_2^2 + 5w_1^4w_2^3 + 5w_1^3w_2^4 + 4w_1^2w_2^5 + 2w_1w_2^6 + w_2^7$
7	3 + 3 + 1	C_{3v}	capped octahedron	$w_1^7 + 3w_1^6w_2 + 7w_1^5w_2^2 + 13w_1^4w_2^3 + 13w_1^3w_2^4 + 7w_1^2w_2^5 + 3w_1w_2^6 + w_2^7$
7	3 + 3 + 1	C_{3v}	capped triangular prism	$w_1^7 + 3w_1^6w_2 + 7w_1^5w_2^2 + 13w_1^4w_2^3 + 13w_1^3w_2^4 + 7w_1^2w_2^5 + 3w_1w_2^6 + w_2^7$
7	3 + 3 + 1	C_{3v}	tri-capped tetrahedron	$w_1^7 + 3w_1^6w_2 + 7w_1^5w_2^2 + 13w_1^4w_2^3 + 13w_1^3w_2^4 + 7w_1^2w_2^5 + 3w_1w_2^6 + w_2^7$
7	2 + 2 + 2 + 1	C_{2v}	4-capped elongated triangular prism	$w_1^7 + 4w_1^6w_2 + 12w_1^5w_2^2 + 19w_1^4w_2^3 + 19w_1^3w_2^4 + 12w_1^2w_2^5 + 4w_1w_2^6 + w_2^7$
8	8	D_{8h}	octagon	$w_1^8 + w_1^7w_2 + 4w_1^6w_2^2 + 5w_1^5w_2^3 + 8w_1^4w_2^4 + 5w_1^3w_2^5 + 4w_1^2w_2^6 + w_1w_2^7 + w_2^8$
8	8	O_h	cube	$w_1^8 + w_1^7w_2 + 3w_1^6w_2^2 + 3w_1^5w_2^3 + 7w_1^4w_2^4 + 3w_1^3w_2^5 + 3w_1^2w_2^6 + w_1w_2^7 + w_2^8$
8	8	D_{4d}	square antiprism	$w_1^8 + w_1^7w_2 + 6w_1^6w_2^2 + 7w_1^5w_2^3 + 13w_1^4w_2^4 + 7w_1^3w_2^5 + 6w_1^2w_2^6 + w_1w_2^7 + w_2^8$
8	7 + 1	C_{7v}	heptagonal pyramid	$w_1^8 + 2w_1^7w_2 + 4w_1^6w_2^2 + 8w_1^5w_2^3 + 10w_1^4w_2^4 + 8w_1^3w_2^5 + 4w_1^2w_2^6 + 2w_1w_2^7 + w_2^8$
8	6 + 2	D_{6h}	hexagonal bipyramid	$w_1^8 + 2w_1^7w_2 + 5w_1^6w_2^2 + 7w_1^5w_2^3 + 10w_1^4w_2^4 + 7w_1^3w_2^5 + 5w_1^2w_2^6 + 2w_1w_2^7 + w_2^8$
8	6 + 2	D_{3h}	bicapped triangular prism	$w_1^8 + 2w_1^7w_2 + 7w_1^6w_2^2 + 10w_1^5w_2^3 + 16w_1^4w_2^4 + 10w_1^3w_2^5 + 7w_1^2w_2^6 + 2w_1w_2^7 + w_2^8$
8	6 + 2	D_{3h}	bicapped octahedron	$w_1^8 + 2w_1^7w_2 + 7w_1^6w_2^2 + 10w_1^5w_2^3 + 16w_1^4w_2^4 + 10w_1^3w_2^5 + 7w_1^2w_2^6 + 2w_1w_2^7 + w_2^8$
8	4 + 4	D_{2h}	parallelopiped	$w_1^8 + 2w_1^7w_2 + 10w_1^6w_2^2 + 14w_1^5w_2^3 + 22w_1^4w_2^4 + 14w_1^3w_2^5 + 10w_1^2w_2^6 + 2w_1w_2^7 + w_2^8$
8	4 + 4	D_{2d}	bidisphenoid	$w_1^8 + 2w_1^7w_2 + 10w_1^6w_2^2 + 14w_1^5w_2^3 + 22w_1^4w_2^4 + 14w_1^3w_2^5 + 10w_1^2w_2^6 + 2w_1w_2^7 + w_2^8$
9	9	D_{9h}	nonagon	$w_1^9 + w_1^8w_2 + 4w_1^7w_2^2 + 7w_1^6w_2^3 + 10w_1^5w_2^4 + 10w_1^4w_2^5 + 7w_1^3w_2^6 + 4w_1^2w_2^7 + w_1w_2^8 + w_2^9$
9	8 + 1	C_{8v}	octagonal pyramid	$w_1^9 + 2w_1^8w_2 + 5w_1^7w_2^2 + 11w_1^6w_2^3 + 17w_1^5w_2^4 + 17w_1^4w_2^5 + 11w_1^3w_2^6 + 5w_1^2w_2^7 + 2w_1w_2^8 + w_2^9$
9	7 + 2	D_{7h}	hept bp	$w_1^9 + 2w_1^8w_2 + 5w_1^7w_2^2 + 8w_1^6w_2^3 + 12w_1^5w_2^4 + 12w_1^4w_2^5 + 8w_1^3w_2^6 + 5w_1^2w_2^7 + 2w_1w_2^8 + w_2^9$
9	3 + 3 + 3	C_{3v}	tricapped octahedron	$w_1^9 + 3w_1^8w_2 + 12w_1^7w_2^2 + 30w_1^6w_2^3 + 42w_1^5w_2^4 + 42w_1^4w_2^5 + 30w_1^3w_2^6 + 12w_1^2w_2^7 + 3w_1w_2^8 + w_2^9$
9	4 + 4 + 1	C_{4v}	capped cube	$w_1^9 + 3w_1^8w_2 + 10w_1^7w_2^2 + 22w_1^6w_2^3 + 34w_1^5w_2^4 + 34w_1^4w_2^5 + 22w_1^3w_2^6 + 10w_1^2w_2^7 + 3w_1w_2^8 + w_2^9$
9	4 + 4 + 1	C_{4v}	capped square antiprism	$w_1^9 + 3w_1^8w_2 + 10w_1^7w_2^2 + 22w_1^6w_2^3 + 34w_1^5w_2^4 + 34w_1^4w_2^5 + 22w_1^3w_2^6 + 10w_1^2w_2^7 + 3w_1w_2^8 + w_2^9$
9	6 + 3	D_{3h}	3-layer triangular prism	$w_1^9 + 2w_1^8w_2 + 8w_1^7w_2^2 + 17w_1^6w_2^3 + 24w_1^5w_2^4 + 24w_1^4w_2^5 + 17w_1^3w_2^6 + 8w_1^2w_2^7 + 2w_1w_2^8 + w_2^9$
10	10	D_{10h}	decagon	$w_1^{10} + w_1^9w_2 + 5w_1^8w_2^2 + 8w_1^7w_2^3 + 16w_1^6w_2^4 + 16w_1^5w_2^5 + 16w_1^4w_2^6 + 8w_1^3w_2^7 + 5w_1^2w_2^8 + w_1w_2^9 + w_2^{10}$
10	10	D_{5d}	bipunctured icosahedron	$w_1^{10} + w_1^9w_2 + 7w_1^8w_2^2 + 12w_1^7w_2^3 + 26w_1^6w_2^4 + 26w_1^5w_2^5 + 26w_1^4w_2^6 + 12w_1^3w_2^7 + 7w_1^2w_2^8 + w_1w_2^9 + w_2^{10}$
10	9 + 1	C_{9v}	nonagonal pyramid	$w_1^{10} + 2w_1^9w_2 + 5w_1^8w_2^2 + 14w_1^7w_2^3 + 24w_1^6w_2^4 + 28w_1^5w_2^5 + 24w_1^4w_2^6 + 14w_1^3w_2^7 + 5w_1^2w_2^8 + 2w_1w_2^9 + w_2^{10}$
10	8 + 2	D_{4h}	bicapped cube	$w_1^{10} + 2w_1^9w_2 + 9w_1^8w_2^2 + 16w_1^7w_2^3 + 33w_1^6w_2^4 + 34w_1^5w_2^5 + 33w_1^4w_2^6 + 16w_1^3w_2^7 + 9w_1^2w_2^8 + 2w_1w_2^9 + w_2^{10}$
10	8 + 2	D_{4d}	bicapped square antiprism	$w_1^{10} + 2w_1^9w_2 + 9w_1^8w_2^2 + 16w_1^7w_2^3 + 33w_1^6w_2^4 + 34w_1^5w_2^5 + 33w_1^4w_2^6 + 16w_1^3w_2^7 + 9w_1^2w_2^8 + 2w_1w_2^9 + w_2^{10}$

Table I (Continued)

n	P_n	G	polyhedron	GF
10	8 + 2	D_{8h}	octagonal bipyramid	$w_1^{10} + 2w_1^9w_2 + 6w_1^8w_2^2 + 10w_1^7w_2^3 + 19w_1^6w_2^4 + 20w_1^5w_2^5 + 19w_1^4w_2^6 + 10w_1^3w_2^7 + 6w_1^2w_2^8 + 2w_1w_2^9 + w_2^{10}$
10	6 + 4	T_d	tetracapped octahedron	$w_1^{10} + 2w_1^9w_2 + 5w_1^8w_2^2 + 14w_1^7w_2^3 + 22w_1^6w_2^4 + 24w_1^5w_2^5 + 22w_1^4w_2^6 + 14w_1^3w_2^7 + 5w_1^2w_2^8 + 2w_1w_2^9 + w_2^{10}$
10	6 + 4	T_d	adamantane	$w_1^{10} + 2w_1^9w_2 + 5w_1^8w_2^2 + 14w_1^7w_2^3 + 22w_1^6w_2^4 + 24w_1^5w_2^5 + 22w_1^4w_2^6 + 14w_1^3w_2^7 + 5w_1^2w_2^8 + 2w_1w_2^9 + w_2^{10}$
12	12	I_h	icosahedron	$w_1^{12} + w_1^{11}w_2 + 3w_1^{10}w_2^2 + 5w_1^9w_2^3 + 12w_1^8w_2^4 + 14w_1^7w_2^5 + 24w_1^6w_2^6 + 14w_1^5w_2^7 + 12w_1^4w_2^8 + 5w_1^3w_2^9 + 3w_1^2w_2^{10} + w_1w_2^{11} + w_2^{12}$

Table II. Isomers of $C_{60}H_n$

no. of isomers	n	no. of isomers	n
1.00000000000000000	0	2493474394140.00000	16
1.00000000000000000	1	6453694644705.00000	17
37.0000000000000000	2	15417163018725.0000	18
577.000000000000000	3	34080036632565.0000	19
8236.00000000000000	4	69864082608210.0000	20
91030.0000000000000	5	133074428781570.000	21
835476.000000000000	6	235904682814710.000	22
6436782.00000000000	7	389755540347810.000	23
42650532.0000000000	8	600873146368170.000	24
246386091.000000000	9	865257299572455.000	25
1256602779.00000000	10	1164769471671687.00	26
5711668755.00000000	11	1466746704458899.00	27
23322797475.0000000	12	1728665795116244.00	28
86114390460.0000000	13	1907493251046152.00	29
289098819780.000000	14	1971076398255692.00	30
886568158468.000000	15		

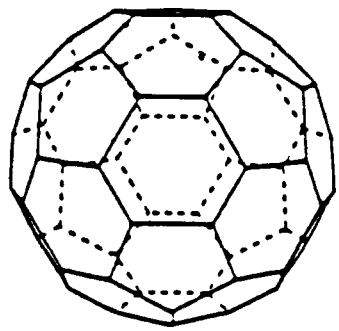

Figure 4. Structure of buckminsterfullerene.

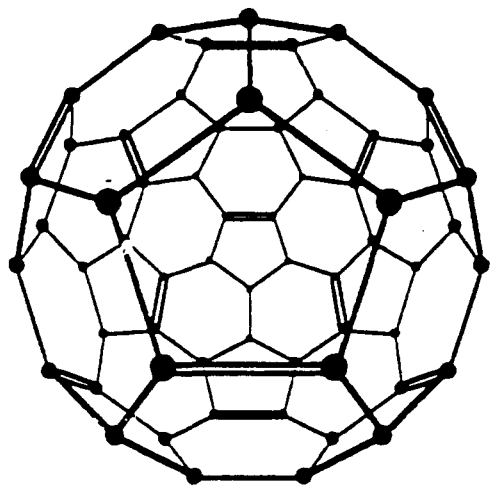

Figure 5. Possible isomer for $C_{60}H_{36}$ generated by the Birch reaction.

computational limitations restrict the set R to contain at most five different colors. Note that white could stand for no substitution, green for hydrogen, blue for deuterium, red for halogen, etc. Let $w(r)$ be a weight which is simply a formal symbol to bookkeep the colorings associated with $r \in R$. Then, the use of GCCI with the identity character yields

$$\mathrm{GF} = P_G[x_k \rightarrow \sum_{r \in R} w(r)^k]$$

Table III. Isomers of $C_{60}H_nD_m$ or $C_{60}H_nCl_m$

no. of isomers	n	m	no. of isomers	n	m
1.00000000000000000	0	1	1119487075980.00000	47	1
59.0000000000000000	1	1	279871768995.000000	48	1
1711.00000000000000	2	1	62828356305.0000000	49	1
32509.0000000000000	3	1	12565671261.0000000	50	1
455126.000000000000	4	1	2217471399.00000000	51	1
5006386.00000000000	5	1	341149446.000000000	52	1
45057474.0000000000	6	1	45057474.0000000000	53	1
341149446.000000000	7	1	5006386.00000000000	54	1
2217471399.00000000	8	1	455126.000000000000	55	1
12565671261.0000000	9	1	32509.0000000000000	56	1
62828356305.0000000	10	1	1711.00000000000000	57	1
279871768995.000000	11	1	59.0000000000000000	58	1
1119487075980.00000	12	1	48981.0000000000000	2	2
4047376351620.00000	13	1	910252.000000000000	3	2
13298522298180.0000	14	1	12519010.0000000000	4	2
39895566894540.0000	15	1	135172422.000000000	5	2
109712808959985.000	16	1	1194050466.00000000	6	2
277508869722315.000	17	1	8869885596.00000000	7	2
647520696018735.000	18	1	56545698807.0000000	8	2
1397281501935165.00	19	1	314141781525.000000	9	2
2794563003870330.00	20	1	1539295620135.00000	10	2
5189902721473470.00	21	1	6716922455880.00000	11	2
8964377427999630.00	22	1	26307949848180.0000	12	2
14420954992868970.0	23	1	93089656087260.0000	13	2
21631432489303455.0	24	1	299216763414900.000	14	2
30284005485024837.0	25	1	877702471679880.000	15	2
39602161018878633.0	26	1	2358825424830765.00	16	2
48402641245296107.0	27	1	16688080.0000000000	3	3
55317304280338409.0	28	1	225287370.000000000	4	3
59132290782430713.0	29	1	2388046122.00000000	5	3
59132290782430713.0	30	1	20696400864.0000000	6	3
55317304280338409.0	31	1	150788055132.000000	7	3
48402641245296107.0	32	1	942425344575.000000	8	3
39602161018878633.0	33	1	5130982438035.00000	9	3
30284005485024837.0	34	1	24628715671560.0000	10	3
21631432489303455.0	35	1	105231785142120.000	11	3
14420954992868970.0	36	1	403388509737300.000	12	3
8964377427999630.00	37	1	1396344841308900.00	13	3
5189902721473470.00	38	1	4388512358399400.00	14	3
2794563003870330.00	39	1	12580402094155800.0	15	3
1397281501935165.00	40	1	2985098760.00000000	4	4
647520696018735.000	41	1	316654915830.000000	5	5
277508869722315.000	42	1	21550129191180.0000	6	6
109712808959985.000	43	1	99218540276850.0000	7	7
39895566894540.0000	44	1	32090996723221800.0	8	8
13298522298180.0000	45	1	749582291439089248	9	9
4047376351620.00000	46	1			

Table IV. GCCIs of the Buckminsterfullerene Cluster[a]

Γ/cycle type	x_1^6	x_5^{12}	x_3^{20}	x_2^{30}	x_{10}^6	x_6^{10}
A_g	1	24	20	31	24	20
T_{1g}	3	12	0	−27	12	0
T_{2g}	3	12	0	−27	12	0
G_g	4	−24	20	4	−24	20
H_g	5	0	−20	15	0	−20
A_u	1	24	20	−1	−24	−20
T_{1u}	3	12	0	−3	12	0
T_{2u}	3	12	0	−3	−12	0
G_u	4	−20	20	−4	24	−20
H_u	5	0	−20	−5	0	20

[a] All cycle indices should be divided by 120.

Table V. Nuclear Spin Statistical Weights of the Rovibronic Levels of $^{13}C_{60}$, $C_{60}H_{60}$, and $C_{60}D_{60}$

rovibronic level	statistical weight[a]	
	$C_{60}H_{60}$	$C_{60}D_{60}$
$A_g(A_u)$	19, 215, 358, 678, 900, 736	706, 519, 304, 586, 988, 199, 183, 738, 259
$T_{1g}(T_{1u})$	57, 646, 074, 961, 907, 712	2, 119, 557, 913, 760, 758, 702, 931, 804, 286
$T_{2g}(T_{2u})$	57, 646, 074, 961, 907, 712	2, 119, 557, 913, 760, 758, 702, 931, 804, 286
$G_g(G_u)$	76, 861, 433, 640, 804, 352	2, 826, 077, 218, 347, 746, 902, 115, 011, 104
$H_g(H_u)$	96, 076, 792, 318, 656, 512	3, 532, 596, 522, 934, 735, 097, 811, 964, 962

[a] The statistical weights of g and u levels are the same. All statistical weights were obtained using quadruple-precision arithmetic on a microvax.

Table VI. Nuclear Spin Statistical Weights of the Rotational Levels of $J = 0$–30^a for $C_{60}H_{60}$ and $C_{60}D_{60}$

J	irreducible representations	statistical wt $\times f^b$
0	A	1
1	T_1	3
2	H	5
3	$T_2 + G$	7
4	$G + H$	9
5	$T_1 + T_2 + H$	11
6	$A + T_1 + G + H$	13
7	$T_1 + T_2 + G + H$	15
8	$T_2 + G + 2H$	17
9	$T_1 + T_2 + 2G + H$	19
10	$A + T_1 + T_2 + G + 2H$	21
11	$2T_1 + T_2 + G + 2H$	23
12	$A + T_1 + T_2 + 2G + 2H$	25
13	$T_1 + 2T_2 + 2G + 2H$	27
14	$T_1 + T_2 + 2G + 3H$	29
15	$A + 2T_1 + 2T_2 + 2G + 2H$	31
16	$A + 2T_1 + T_2 + 2G + 3H$	33
17	$2T_1 + 2T_2 + 2G + 3H$	35
18	$A + T_1 + 2T_2 + 3G + 3H$	37
19	$2T_1 + 2T_2 + 3G + 3H$	39
20	$A + 2T_1 + 2T_2 + 2G + 4H$	41
21	$A + 3T_1 + 2T_2 + 3G + 3H$	43
22	$A + 2T_1 + 2T_2 + 3G + 4H$	45
23	$2T_1 + 3T_2 + 3G + 4H$	47
24	$A + 2T_1 + 2T_2 + 4G + 4H$	49
25	$A + 3T_1 + 3T_2 + 3G + 4H$	51
26	$A + 3T_1 + 2T_2 + 3G + 5H$	53
27	$A + 3T_1 + 3T_2 + 4G + 4H$	55
28	$A + 2T_1 + 3T_2 + 4G + 5H$	57
29	$3T_1 + 3T_2 + 4G + 5H$	59
30	$2A + 3T_1 + 3T_2 + 4G + 5H$	61

[a] The irreducible representations for $J > 31$ are given in $q(A + 3T_1 + 3T_2 + 4G + 5H) + \Gamma(r)$, where q is the quotient obtained by dividing J by 30, and r is the remainder. $\Gamma(r)$ is the set of irreducible representations spanned by $J = r$ listed in this table (see text for further discussion). Note that since nuclear spin statistical weights are the same for g and u symmetries we do not show g or u. [b] $f = 19, 215, 358, 678, 900, 736$ for $C_{60}H_{60}$. $f = 706, 519, 304, 586, 988, 199, 183, 738, 259$ for $C_{60}D_{60}$.

Suppose the set R contains two types of colors say white (no substitution) and green (hydrogen). Then the following GF is obtained

$$GF^2 = 1/60[(1 + w)^{60} + 24(1 + w^5)^{20} + 20(1 + w^3)^{20} + 15(1 + w^2)^{30}]$$

The coefficient of w^n in the above expression then generates isomers of $C_{60}H_n$. Consider a GF for the case wherein the set R contains four colors say white, green, blue, and yellow with weights 1, w_1, w_2, and w_3, respectively. The GF for this case is more complex and is given by

$$GF^4 = 1/60[(1 + w_1 + w_2 + w_3)^{60} + 24(1 + w_1^5 + w_2^5 + w_3^5)^{12} + 20(1 + w_1^3 + w_2^3 + w_3^3)^{20} + 15(1 + w_1^2 + w_2^2 + w_3^2)^{30}]$$

To illustrate, the coefficient of say $w_1^{20}w_2^{10}w_3^{10}$ in the above expression generates the number of isomers of $C_{60}H_{20}F_{10}Cl_{10}$.

The computational complexity of computing the coefficients in the GF grows as the number of elements in the set R increases since the evaluation of a general coefficient $w_1^{b_1}w_2^{b_2} \ldots w_n^{b_n}$ involves multinomial expansions. The coefficient of $w_1^{b_1}w_2^{b_2} \ldots w_m^{b_m}$ in the expansion $(1 + w_1 + w_2 + \ldots w_m)^n$ is given by

$$\binom{n}{1b_1b_2 \ldots b_m} = \frac{n!}{b_1!b_2! \ldots b_m!}$$

For large values of n or $b_1, b_2 \ldots b_m$ the factorials of those numbers grow to large values, making computation of the isomer numbers impossible if this technique of evaluating multinomial numbers is used.

I designed a computational algorithm which overcomes the computational overflow bottlenecks introduced by the conventional procedures for computing multinomial numbers involving large factorials. This algorithm was implemented in quadruple precision arithmetic in ref and was tested for several cases.

The total number of all isomers is obtained by replacing all x_k to $|R|$, the number of elements in the set R. Hence the total number of isomers of $C_{60}H_n$ for all n is given by

$$N = 1/60[2^{60} + (24 \times 2^{12}) + (20 \times 2^{20}) + (15 \times 2^{30})]$$

Likewise, the total number of isomers of $C_{60}H_mD_n$ for all possible m and n is given by

$$N = 1/60[3^{60} + (24 \times 3^{12}) + (20 \times 3^{20}) + (15 \times 3^{30})]$$

Table II shows the number of isomers for $C_{60}H_n$ for n = 0–30 obtained on a microvax computer. In Table II only the first 30 coefficients are shown due to the symmetry of binomial numbers. That is, for example, the coefficient for $n = 31$ is same as the coefficient for $n = 29$. In general, the coefficient of $n + 30$ in Table I is the same as the coefficient of $30 - n$ for n = 1–30.

The coefficient for $n = 1$ is 1 (Table II), in accord with the single-line-observed n the NMR spectra of C_{60}^3 since the number of NMR signals is the coefficient of w in the GF as formulated in a previous paper.[30] It is interesting to note that there are 37 possible isomers for $C_{60}H_2$ and 577 for $C_{60}H_3$, etc. Recent theoretical computations reveal that some hydrogens prefer to be inside the soccerball to minimize energies.

Particular cases of recent experimental interest[20] are $C_{60}H_{36}$ and $C_{60}H_{60}$. One such isomer of $C_{60}H_{36}$ proposed by Smalley and co-workers[20] is shown in Figure 5. The reason for the stability of this isomer is that 36 hydrogens are required to leave a single unconjugated double bond in each pentagon of C_{60} so as to preserve the lack of conjugation. The isomer generated in the Birch reduction is supposed to attack mainly conjugated double bonds. At the present time it is not completely established if this is the only most stable isomer for $C_{60}H_{36}$ or if among 600 873 146 368 170 isomers possible for $C_{60}H_{36}$ several isomers could be stable. It is possible that the particular way the Birch reduction is made may lead to this isomers since the Birch reduction is very selective.

Table III shows the possible isomers of $C_{60}H_nD_m$ as well as $C_{60}H_nX_m$ (X = F, Cl). There are 59 possible isomers for $C_{60}HF$ and $C_{60}HD$. Likewise there exists 1711 and 32507 isomers for $C_{60}H_2D$ and $C_{60}H_3D$, respectively. The number of isomers of $C_{60}H_2D_2$ is 48981 ($m = 2$, and $n = 2$).

Possible applications to multiple quantum NMR spectra of randomly deuterated $C_{60}H_n$ were considered.[30] It remains to be seen if such multiple quantum NMR spectra can be recorded.

5. ROTATIONAL LEVELS AND NUCLEAR SPIN STATISTICS OF $^{13}C_{60}$, $C_{60}H_{60}$, AND $C_{60}D_{60}$

I[31] recently applied the GCCI combinatorial method to compute the nuclear spin statistical weights of the rotational levels of the title molecules in this section. The analysis of the intensity patterns of high-resolution spectra requires information on the nuclear spin statistical weights of rotational (rovibronic) levels. The combinatorics of the problem involve 2^{60} or 3^{60} possible spin functions. The ratio of the nuclear spin statistical weights would provide manageable information on the intensity ratios of the observed transitions.

The GCCIs of all irreducible representations of the I_h group are shown in Table IV. It was shown that the nuclear spin statistical weights are the same for both I_h and I rotational subgroups.

The GCCIs in this case yield generating functions for nuclear spin species upon replacing every x_k by $\alpha^k + \beta^k$ if α denotes spin up an β denotes spin down for $C_{60}H_{60}$ and $^{13}C_{60}$. Equivalently

$$GF^{\chi} = P^{\chi}_{G}(x_k \rightarrow \alpha^k + \beta^k)$$

The generating function for the deuterated $C_{60}D_{60}$ is given by

$$GF^{\chi} = P^{\chi}_{G}(x_k \rightarrow \lambda^k + \mu^k + \nu^k)$$

where λ, μ, and ν are the three possible z-projections for the deuterium nuclear spin.

The number of times the irreducible representation Γ with character $\chi: g \rightarrow \chi(g)$ occurs in the set of all protonic or ^{13}C spin functions is given by

$$n_{\Gamma} = P^{\chi}_{G}(x_k \rightarrow 2)$$

where every x_k is replaced by 2 since there are two possible spin projections for the hydrogen nucleus or the ^{13}C nucleus. Likewise, the number of times the irreducible representation Γ occurs in the set of all deuterated spin functions is given by

$$n_{\Gamma} = P^{\chi}_{G}(x_k \rightarrow 3)$$

For example, the number of times the T_1 representation occurs in the set of all 2^{60} protonic spin functions is directly given by

$$n_{T_1} = 1/120[3.2^{60} + 12.2^{12} - 27.2^{30} - 27.2^{30} + 12.2^{6}]$$

Table V shows the final nuclear spin statistical weights for $^{13}C_{60}$, $C_{60}H_{60}$, and $C_{60}D_{60}$ obtained using double-precision and quadruple-precision real arithmetic, respectively. They were obtained by stipulating that the direct product of the rovibronic species and nuclear spin species be antisymmetric since ^{13}C and H nuclei are fermions. Since all the operations of the I group yield either even permutations of nuclei or even numbers of odd permutations, the overall species is A_g or A_u for the I_h group. The nuclear spin statistical weights were obtained by stipulating that

$$\Gamma^{rve} \otimes \Gamma^{spin} \subset A_g \text{ or } A_u$$

The ratio of the nuclear spin statistical weights of the rovibronic levels of A_g, T_{1g}, T_{2g}, G_g, and H_g symmetries (Table V) is approximately 1:3:3:4:5. Since the intensity ratios depend on the ratio of the spin statistical weights, it is interesting that in the final ratio, the large nuclear spin statistical weight of the A_g level is (approximately) factored out.

Table VI shows the correlation table for the rotational levels with J = 0–30 in the I point group and their nuclear spin statistical weights of the rotational levels in the factored form. Harter and Weeks[41] as Balasubramanian et al.[42] have also obtained correlation of $D^{(J)}$ to I_h. Table VI contains results up to J = 30 since $J > 30$ can be readily derived from results up to J = 30 (see refs 31 and 41 for details).

REFERENCES AND NOTES

(1) O'Brien, S. C.; Liu, Y.; Zhang, Q.; Heath, J. R.; Tittel, F. K.; Curl, R. F.; Smalley, R. E. Supersonic Cluster Beams of III–V Semiconductors: Ga_xAs_y. *J. Chem. Phys.* **1986**, *84*, 4074.
(2) Zhang, Q. L.; Liu, Y.; Curl, R. F.; Tittle, F. K.; Smalley, R. E. Photodissociation of Semiconductor Positive Cluster Ions. *J. Chem. Phys.* **1988**, *86*, 1670.
(3) Balasubramanian, K. Spectroscopic Properties and Potential Energy Curves of Heavy p-Block Dimers and Trimers. *Chem. Rev.* **1990**, *90*, 93.
(4) Morse, M. D. Clusters of Transition-Metal Atoms. *Chem. Rev.* **1986**, *86*, 1046.
(5) (a) Phillips, J. C. Chemical Bonding, Kinetics, and the Approach to Equilibrium Structure of Simple Metallic, Molecular and Network Microclusters. *Chem. Rev.* **1986**, *86*, 619. (b) Mandich, M. L.; Reents, W. D., Jr.; Bondybey, V. E. In *Atomic and Molecular Clusters*; Bernstein, E. R., Ed.; Elsevier: Amsterdam, 1990.
(6) Kroto, H. W.; Heath, J. R.; O'Brien, S. C.; Curl, R. F.; Smalley, R. E. C_{60}: Buckminsterfullerene. *Nature* **1985**, *318*, 162.
(7) Liu, Y.; O'Brien, S. C.; Zhang, Q.; Liu, Y.; Curl, R. F.; Kroto, H. W.; Tittle, F. K.; Smalley, R. E. Negative Carbon Cluster Ion Beams: New Evidence for the Special Nature of C_{60}. *Chem. Phys. Lett.* **1986**, *126*, 215.
(8) Heath, J. R.; O'Brien, S. C.; Zhang, Q.; Liu, Y.; Curl, R. F.; Kroto, H. W.; Tittle, F. K.; Smalley, R. E. Lanthanum Complexes of Spheroidal Carbon Shells. *J. Am. Chem. Soc.* **1985**, *107*, 7779.
(9) Klein, D. J.; Schmalz, T. G.; Hite, G. F.; Seitz, W. A. Icosahedral Symmetry Carbon Cage Molecules. *Nature* **1986**, 703.
(10) Stone, A. J.; Wales, D. J. Theoretical Studies of Icosahedral C_{60} and Some Related Species. *Chem. Phys. Lett.* **1986**, *128*, 501.
(11) Klein, D. J.; Seitz, W. A.; Schmalz, T. G. C_{60} Carbon Cages. *Chem. Phys. Lett.* **1986**, *130*, 203.
(12) Haymet, A. D. H. C_{120} and C_{60}: Archimedean Solids Constructed from sp^2 Hybridized Atoms. *Chem. Phys. Lett.* **1985**, *122*, 421.
(13) Davidson, R. A. Spectral Analysis of Graphs by Cyclic Automorphism Subgroups. *Theor. Chim. Acta* **1981**, *58*, 193.
(14) Elser, V.; Haddon, R. C. Icosahedral C_{60}: An Aromatic Molecule with a Vanishingly Small Ring Current Magnetic Susceptibility. *Nature* **1987**, *325*, 792.
(15) Mallion, R. B. Ring-Current Effects in C_{60}. *Nature* **1987**, *325*, 700.
(16) Shibuya, T.; Yoshitani, M. Two Icosahedral Structures for C_{60} Clusters. *Chem. Phys. Lett.* **1987**, *137*, 13.
(17) Balasubramanian, K.; Liu, X. Y. Computer Generation of Spectra of Graphs. Applications to C_{60} Clusters and Other Systems. *J. Comput. Chem.* **1988**, *4*, 406.
(18) Balasubramanian, K.; Liu, X. Y. Spectra and Characteristic Polynomials of Polyhedral Clusters. *Int. J. Quantum Chem., Quantum Chem. Symp.* **1988**, *22*, 319.
(19) Dias, J. A Facile Hückel Molecular Orbital Solution of Buckminsterfullerene Using Chemical Graph Theory. *J. Chem. Educ.* **1989**, *66*, 1012.
(20) Haufler, R. E.; Conceicao, J.; Chibante, L. P. F.; Chai, Y.; Byrne, N. E.; Flanagan, S.; Hayley, M. M.; O'Brien, S. C.; Pan, C.; Xiao, Z.; Billups, W. E.; Ciufolini, M. A.; Hauge, R. H.; Margrave, J. L.; Wilson, L. J.; Curl, R. F.; Smalley, R. E. Efficient Production of C_{60} (Buckminsterfullerene), $C_{60}H_{36}$, and the Solvated Buckide Ion. *J. Phys. Chem.* **1990**, *94*, 8634.
(21) Kratschmer, W.; Fostiropoulous, K.; Huffman, D. R. The Infrared and Ultraviolet Absorption Spectra of Laboratory-Produced Carbon Dust: Evidence for the Presence of the C_{60} Molecule. *Chem. Phys. Lett.* **1990**, *170*, 167.
(22) Johnson, R. D.; Meijer, G.; Bethune, D. S. *J. Am. Chem. Soc.*, in press.
(23) Balasubramanian, K. Spectral Moments and Walks for Large Carbon Clusters. *Chem. Phys. Lett.* **1990**, *175*, 273.
(24) Balasubramanian, K. Computer Generation of Walks and Self-Returning Walks on Chemical Graphs. *Comput. Chem.* **1985**, *9*, 43.
(25) Balasubramanian, K. Applications of Combinatorics and Graph Theory to Spectroscopy and Quantum Chemistry. *Chem. Rev.* **1985**, *85*, 599.
(26) Balasubramanian, K. A Generalized Wreath Product Method for the Enumeration of Stereo and Position Isomers of Polysubstituted Organic Compounds. *Theor. Chim. Acta* **1979**, *51*, 37.
(27) Balasubramanian, K. Computer Generation of Isomers. *Comput. Chem.* **1982**, *6*, 57.
(28) Pólya, G. Kombinatorische Anzahlbestimmunger für Gruppen, Graphen und Chemische Verbindungen. *Acta Math.* **1937**, *65*, 145.
(29) Balasubramanian, K. Computer-Assisted Enumeration of NMR Signals. *J. Magn. Reson.* **1982**, *48*, 165.
(30) Balasubramanian, K. Enumeration of Isomers of Polysubstituted C_{60} and Application to NMR. *Chem. Phys. Lett.*, in press.
(31) Balasubramanian, K. Nuclear Spin Statistics of C_{60}, $C_{60}H_{60}$, and $C_{60}D_{60}$. *Chem. Phys. Lett.*, in press.
(32) Balasubramanian, K. Enumeration of Isomers of Gallium Arsenide Clusters. *Chem. Phys. Lett.* **1988**, *150*, 71.
(33) Balasubramanian, K. Spectroscopic Constants and Potential Energy Curves of 47 Electronic States of InSb, $InSb^+$, and $InSb^-$. *Chem. Phys. Lett.* **1990**, *93*, 507.
(34) Reents, W. D., Jr. Relative Etching of $Ga_xAs_y^-$ by HCl. *J. Chem. Phys.* **1989**, *90*, 4258.
(35) Kolenbrander, K. D.; Mandich, M. Optical and Near-Infrared Spec-

troscopy of Neutral Indium Phosphide Clusters. *J. Chem. Phys.* **1990**, *92*, 4759.
(36) Balasubramanian, K. A Method for Nuclear Spin Statistics in Molecular Spectroscopy. *J. Chem. Phys.* **1981**, *74*, 6824.
(37) Balasubramanian, K. Generating Functions for the Nuclear Spin Statistics of Non-Rigid Molecules. *J. Chem. Phys.* **1981**, *75*, 4572.
(38) King, R. B. Chemical Applications of Topology and Group Theory. XXII: Lowest Degree Chirality Polynomial for Regular Polyhedra. *J. Math. Chem.* **1987**, *1*, 45.
(39) King, R. B. Graph Theory and Topology in Chemistry. *Stud. Phys. Theor. Chem.* **1987**, *51*, 325.
(40) Meier, U.; Peyerimhoff, S. D.; Grein, F. Ab initio MRD-CI Study of $GaAs^-$, $GaAs_2^{(\pm)}$, $Ga_2As_2^{(\pm)}$, $As_2^{(\pm)}$, and As_4 Clusters. *Chem. Phys.* **1989**, *90*, 4727.
(41) Harter, W. G.; Weeks, D. E. Rotation-Vibration Spectra of Icosahedral Molecules. I. Icosahedral Symmetry Analysis and Fine Structure. *J. Chem. Phys.* **1989**, *90*, 4727.
(42) Balasubramanian, K.; Pitzer, K. S.; Strauss, H. L. Nuclear Spin Statistics of Cubane and Icosahedral Borohydride Ions. *J. Mol. Spectrosc.* **1982**, *93*, 447.

Chemical Graph-Theoretical Cluster Expansion and Diamagnetic Susceptibility†

T. G. SCHMALZ, D. J. KLEIN,* and B. L. SANDLEBACK

Texas A&M University at Galveston, Galveston, Texas 77553-1675

Received September 26, 1991

A general computationally amenable chemical graph-theoretical cluster expansion method is described and illustrated in application to the treatment of magnetic susceptibilities. The "additive" cluster expansion in terms of molecular fragments is found to entail certain linear "near-dependences" of graph-theoretical invariants, again as illustrated for magnetic susceptibilities. The general implementation and efficacy of the method are commented upon.

1. CHEMISTRY AND GRAPH THEORY

Chemical graph theory[1] offers a mathematical framework for classical chemical-bonding ideas, here illustrated in application to the description of the magnetic susceptibilities of organic molecules comprised from C, H, and O atoms. We view *chemical graphs* to be mathematical graph-theoretical precepts. A graph is specified in terms of two sets: first, a set of *sites* (or vertices), here identifying atoms in a molecule; and second, a set of edges, each often viewed as site pairs and here identified as chemical bonds. We do however (ultimately) suppress H atoms, assuming that whatever apparent deficit there is in valence (of C or O) is understood to be thus augmented by the requisite number of H atoms. (That is, we avoid radicals.) Double bonds are identified as such. A *subgraph* G' of a graph G is simply a graph whose site and edge sets are subsets of G; this relation is denoted $G' \subset G$.

Graphs as defined here, and elsewhere,[1] are *labeled*, and one often removes the individual site labels to speak of isomorphism classes of graphs. Of course for chemical purposes, the labels should generally not be completely removed so that one still distinguishes atoms of different elements, and we speak of *chemical* isomorphism classes of graphs. Hence one arrives at the "valence structures" of classical chemistry. For instance, for hydroxylamine the three graphs of Figure 1a are chemically isomorphic and form one chemical isomorphism class. The three graphs of Figure 1b are the same (graphs) as those of Figure 1a, and together form the same chemical isomorphism class, denoted in Figure 1c. The four different (connected) two-atom subgraphs of the first graph in Figure 1a (or Figure 1b) are shown in Figure 1d, where the first two form a chemical isomorphism class of subgraphs.

Molecular properties often may be illuminatingly expressed as derived from the various component fragments of a molecule via a formal[2] chemical graph-theoretical cluster expansion. This expansion in an "additive" format[2-5] is described in Section 2, when a molecular property is expressed as a sum of graph-theoretical invariants (these here being counts of certain types of molecular fragment subgraphs). In Section 3 we go on to display examples of linear "near-dependences" among the graph invariants. This feature, already addressed by Essam et al.,[5] is generally derived for the type of cluster expansion discussed here. The ideas (of Sections 2 and 3) are illustrated in Section 4 for the case of magnetic susceptibilities, thereby extending classical Pascal constant ideas,[6] and also recasting "Hameka" magnetic-susceptibility expansions[7,8] into what we believe is a more useful form, as also earlier suggested in a more-limited context by Randić,[9] though more generally in unpublished works.

† Research supported by the Welch Foundation of Houston, TX.

2. CLUSTER EXPANSION

A molecular property $X(\Gamma)$ for a molecule with graph Γ is to be expressed in terms of contributions $x(G)$ for connected subgraphs $G \subset \Gamma$. The general (additive) *cluster expansion* then is[2-4]

$$X(\Gamma) = \sum_{G \in C(\Gamma)} x(G) \tag{2.1}$$

where $C(\Gamma)$ is a set of connected subgraphs of Γ and $x(G)$ are fragment contributions. If we denote the number of subgraphs of Γ chemically isomorphic to G by $n_\Gamma[G]$, then eq 2.1 may be recast as

$$X(\Gamma) = \sum_{[G] \in C[\Gamma]} x(G) n_\Gamma[G] \tag{2.2}$$

where now the sum goes only over chemical isomorphism classes. For instance, hydroxylamine of Figure 1 has

$$n_\Gamma[\mathrm{H}] = 3 \quad n_\Gamma[\mathrm{N}] = n_\Gamma[\mathrm{O}] = 1 \quad n_\Gamma[\mathrm{H\text{-}N}] = 2$$
$$n_\Gamma[\mathrm{N\text{-}O}] = n_\Gamma[\mathrm{O\text{-}H}] = 1 \quad n_\Gamma[\mathrm{H\text{-}N\text{-}O}] = 2 \tag{2.3}$$
$$n_\Gamma[\mathrm{H\text{-}N\text{-}H}] = 1$$
$$n_\Gamma[\mathrm{H\text{-}N\text{-}O\text{-}H}] = 2 \quad n_\Gamma[\mathrm{H_2N\text{-}O}] = 1 \quad n_\Gamma[\Gamma] = 1$$

Of course, the full-cluster expansion of eqs 2.1 or 2.2 is exact. Approximations arise with the truncation of these expansions, say at subgraphs of a limited size. One simple *size measure* (of several possibilities[2]) is the number $|G|$ of vertices in G. Such truncated expansions are common, e.g., for magnetic susceptibilities with atomic contributions (and

0095-2338/92/1632-0054$03.00/0